JOURNAL OF MATERIALS SCIENCE 31 (1996) 5697–5700

Carbon monoxide oxidation on $(Mg_{6-x}Al_x)MnO_8$ $(0 \leqslant x \leqslant 0.6)$

H. TAGUCHI*, A. OHOTA, M. NAGAO
Research Laboratory for Surface Science, Faculty of Science, Okayama University, Okayama 700, Japan

Murdochite-type $(Mg_{6-x}Al_x)MnO_8$ $(0 \leqslant x \leqslant 0.6)$ was synthesized at low temperature (700 °C) with the sol–gel process. The specific surface area, crystallite size, catalytic activity for the CO oxidation, and adsorption isotherms of oxygen on $(Mg_{6-x}Al_x)MnO_8$ were measured. The increase of the specific surface area with increasing Al^{3+} ion content was explained by the decrease of the particle size. The catalytic activity increased with increasing Al^{3+} ion content, and this increase was caused by the valence deviation from the Mn^{4+} ion to the $Mn^{3.5+}$ ion.

1. Introduction

Murdochite-type Mg_6MnO_8 is considered to be derived from the rock salt structure of MgO by replacing one-eighth of the Mg^{2+} ions with Mn^{4+} ions and one-eighth with vacancies [1]. The Mn^{4+} ions and vacancies occupy (1 1 1) alternate lattice layers, and are ordered within the layers. Both the Mg^{2+} and the Mn^{4+} ions are octahedrally co-ordinated by six oxygen ions. Mg_6MnO_8 has a weak ferromagnetic interaction with a Weiss constant, θ, of -20 ± 5 K [2]. The effective magnetic moment, μ_{eff}, in the paramagnetic region is $3.94 \pm 0.08\ \mu_B$, and this value agrees with the spin only value calculated for a $3d^3$ ion in the octahedral configuration ($3.87\ \mu_B$).

By substituting the Al^{3+} ions in Mg_6MnO_8 for the Mg^{2+} ions, Taguchi *et al.* [3] synthesized murdochite-type $(Mg_{6-x}Al_x)MnO_8$. The cell constants monotonically decrease with increasing Al^{3+} ion content. From the results of the magnetic measurement, $(Mg_{6-x}Al_x)MnO_8$ is antiferromagnet and follows the Curie–Weiss law. The effective magnetic moment, μ_{eff}, calculated from the linear portion of the $1/\chi$–T curves is independent of the composition. These results suggest that both the low-spin and the high-spin states of Mn^{3+} ions coexist.

Cimino and Indovina [4] measured the decomposition of N_2O over $MgO–MnO_x$ and $MgO–MnO_x–Li_2O$ catalysts [4]. Pure α-Mn_2O_3 and Mg_6MnO_8 were also tested. Although Mg_6MnO_8 can decompose N_2O, the catalytic activity of Mg_6MnO_8 is lower than α-Mn_2O_3. From these results, it is considered that the Mn^{3+} ions are more active in N_2O decomposition than the Mn^{4+} ions.

In the present study, we synthesized $(Mg_{6-x}Al_x)MnO_8$ at low temperature with the sol–gel process. The specific surface area, the catalytic activity for the carbon monoxide (CO) oxidation, and the adsorption isotherms of oxygen on $(Mg_{6-x}Al_x)MnO_8$ were measured. These results will provide some information on the $(Mg_{6-x}Al_x)MnO_8$ surface and the mechanism of CO oxidation on $(Mg_{6-x}Al_x)MnO_8$.

2. Experimental procedure

$(Mg_{6-x}Al_x)MnO_8$ $(0 \leqslant x \leqslant 0.6)$ was synthesized with the sol–gel process. $Mg(CH_3COO)_2 \cdot 4H_2O$, $Al(NO_3)_3 \cdot 9H_2O$ and $Mn(CH_3COO)_2 \cdot 4H_2O$ powders were weighed in the appropriate proportions and dissolved in distilled water (30 cm^3) at room temperature. The solution was mixed and evaporated in a rotary evaporator at 40–60 °C. The gel was calcined at 400 °C for 2 h in air, then fired at 700 °C for 6 h in air.

The phases of the samples were identified by X-ray powder diffraction (XRD) with monochromatized CuK_α radiation. The crystallite size of the samples was calculated from the half-width of a diffraction peak with Scherrer's equation.

The specific surface area of the samples was determined by the BET method for nitrogen adsorption. The catalytic activity for the CO oxidation was measured at 270–390 °C with the conventional flow system. The samples (0.1 g) were preheated at 300 °C in a pure oxygen stream for 2 h. A mixed gas of CO (1%), O_2 (4%) and He (balance) was fed in the flow reactor at a flow rate of 150 $cm^3\ min^{-1}$. The products were analysed by gas chromatography with a column (molecular sieve 5A) kept at 50 °C during the measurement. The adsorption isotherms of oxygen on the samples were measured at 300 °C with a conventional volumetric adsorption apparatus.

3. Results and discussion

Transparent gel was formed by mixing the acetate aqueous solution. The gel was fired at 700 °C in air for

---

* Author to whom all correspondence should be addressed.

0022–2461 © *1996 Chapman & Hall*

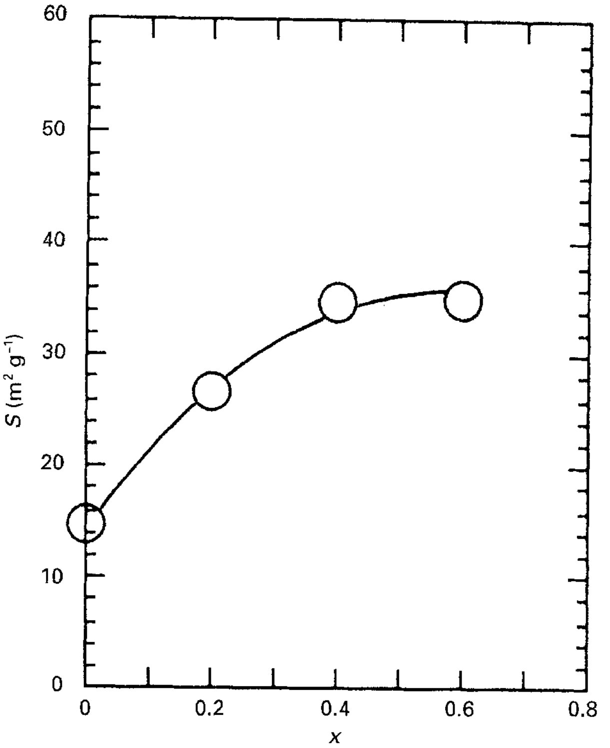

Figure 1 Specific surface area, S, versus composition, x, for $(Mg_{6-x}Al_x)MnO_8$.

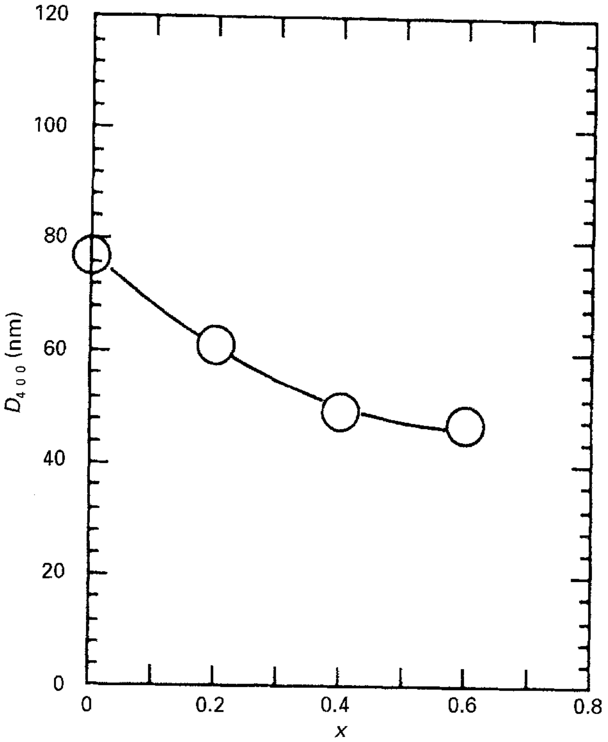

Figure 2 Crystallite size, D_{400}, versus composition, x, for $(Mg_{6-x}Al_x)MnO_8$.

6 h. In the range $0 \leqslant x \leqslant 0.6$, XRD patterns of the fired samples were completely indexed as the cubic murdochite-type structure. Mg_6MnO_8 has generally been synthesized above 900 °C with a solid-state reaction. Although the molar ratio of Mg/Mn in the starting materials was stoichiometric (6/1), the XRD pattern showed a mixture of Mg_6MnO_8 and MgO [1, 2]. For this reason, excess magnesium oxide or magnesium acetate was generally used to synthesize Mg_6MnO_8. Excess MgO in the sample was removed by washing with a hot 10% solution of NH_4Cl. Recently, Taguchi and Nagao [5] reported the synthesis of Mg_6MnO_8 with the sol–gel process. Mg_6MnO_8 was easily synthesized at low temperature from the stoichiometric molar ratio of Mg/Mn. In the present study, the sol–gel process was a useful method to synthesize $(Mg_{6-x}Al_x)MnO_8$ $(0 \leqslant x \leqslant 0.6)$.

Fig. 1 shows the relation between the specific surface area of the samples and the composition. Although all samples were synthesized at 700 °C, the specific surface area was about 14.7 m^2 g^{-1} for $x = 0$ and increased monotonically to about 35.0 m^2 g^{-1} for $x = 0.6$. Taguchi *et al.* [6] reported the surface characterization of perovskite-type $(La_{1-x}Sr_x)MnO_3$ synthesized with the sol–gel process and the solid-state reaction. The specific surface area was about 19.8 m^2 g^{-1} for $LaMnO_3$ $(x = 0)$ synthesized with the sol–gel process, and was independent of the composition. In the present system, the crystallite size, D, of the samples was calculated from the 400 peak and is shown in Fig. 2. D_{400} was about 76.7 nm for $x = 0$ and decreased monotonically to about 47.1 nm for $x = 0.6$. The decrease of D_{400} suggests that the particle size of the samples decreased with increasing Al^{3+} ion content. Consequently, the specific surface area of the samples increased, as shown in Fig. 1.

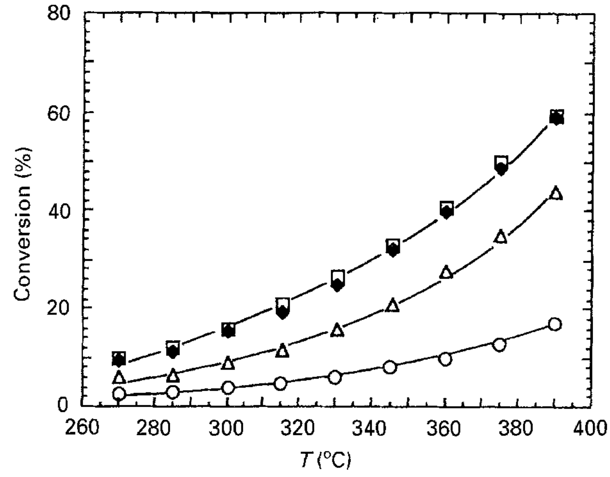

Figure 3 Temperature dependence of the conversion from CO to CO_2 on $(Mg_{6-x}Al_x)MnO_8$. (○) 0, (△) 0.2, (□) 0.4, (◆) 0.6.

The conversion from CO to CO_2 was measured at 270–390 °C with the conventional flow system. Fig. 3 shows the temperature dependence of the conversion. In the range $0 \leqslant x \leqslant 0.4$, the conversion increased with increasing Al^{3+} ion content. We could not find a large difference in the conversion between $x = 0.4$ and 0.6. From the results of Figs 1 and 3, it is obvious that the variation of the conversion corresponds to the specific surface area of the samples. The rate of reaction, R, at a given temperature was calculated from the following equation [7]

$$R = \frac{FCC_v}{mS} \qquad (1)$$

where F is the gas flow per minute, C the initial concentration of CO, C_v the conversion per gram from CO to CO_2, m is the mass of the sample, and S the

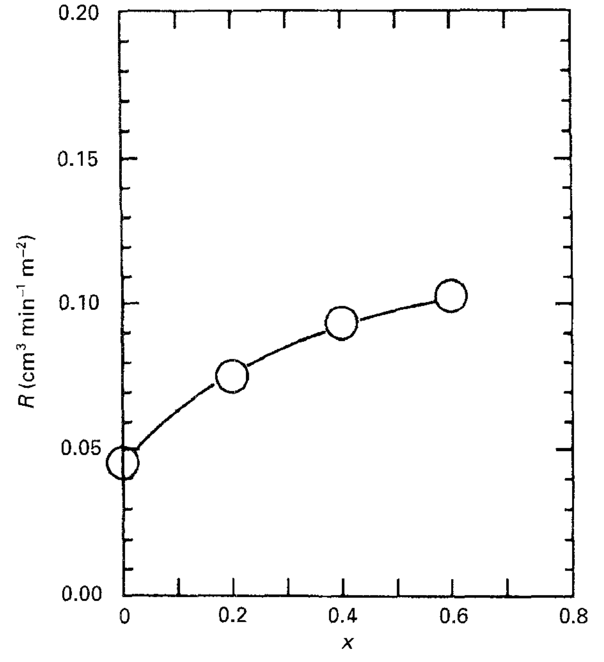

Figure 4 Catalytic activity, R, versus composition, x, for $(Mg_{6-x}Al_x)MnO_8$. The rate of reaction was calculated from the conversion at 300 °C.

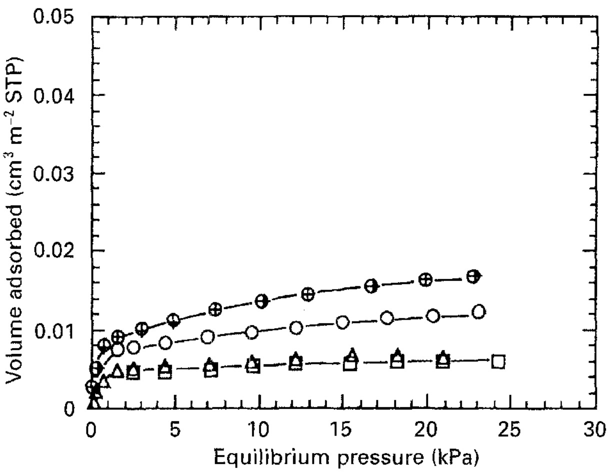

Figure 5 Adsorbed isotherms of oxygen on $(Mg_{6-x}Al_x)MnO_8$ at 300 °C. x: (⊕) 0, (○) 0.2, (□) 0.4, (△) 0.6.

specific surface area of the samples. Fig. 4 shows the relation between the rate of reaction at 300 °C and the composition. The rate of reaction was about $0.046\,cm^3 \cdot min^{-1} \cdot m^{-2}$ for $x = 0$ and increased monotonically to about $0.103\,cm^3 \cdot min^{-1} \cdot m^{-2}$ for $x = 0.6$. These results suggest that the catalytic activity for CO oxidation on $(Mg_{6-x}Al_x)MnO_8$ increases with increasing Al^{3+} ion content.

The adsorption isotherms of oxygen on the samples were measured at 300 °C. Fig. 5 shows the relation between the volume of adsorbed oxygen and the equilibrium pressure. The volume of adsorbed oxygen was small and slightly decreased with increasing Al^{3+} ion content. Table I shows the amount of adsorbed oxygen on the samples. The amount of adsorbed oxygen was calculated from the B-point of the adsorption isotherms of oxygen, and was about $0.27\,mol\,nm^{-2}$ for $x = 0$, and slightly decreased to about $0.14\,mol\,nm^{-2}$. This result suggests that oxygen prefers the sites of the Mn^{4+} ions to the sites of the Mn^{3+} ions.

TABLE I The amount of adsorbed oxygen on $(Mg_{6-x}Al_x)MnO_8$

x	Amount of absorbed oxygen (mol nm^{-2})
0	0.27
0.2	0.21
0.4	0.14
0.6	0.14

The catalytic activity for CO oxidation on the perovskite-type oxides was reported by many researchers [8–13]. CO oxidation occurs at the metal ions of the surface, and the catalytic activity is correlated with the occupation of 3d levels. According to Voorhoeve *et al.* [8], the catalytic activity had the maximum value at the average valence of the metal ions with $(d\varepsilon)^3(d\gamma)^0$ and $(d\varepsilon)^3(d\gamma)^1$ or with $(d\varepsilon)^6(d\gamma)^0$ and $(d\varepsilon)^5(d\gamma)^1$. In such a case, the occupation of the dγ levels is less than one electron, the dε levels being half or totally filled, and the catalytic activity has a maximum value [9]. CO is bonded to the transition metal ions of the surface as a carbonyl, and donates the lone pair of carbons into the empty d_{z^2} orbital of the metal ions to form the σ-bond. At the same time, the back donation of the dε electrons of the metal ions makes the antibonding π-orbital of CO. Because the d_{z^2} orbital is the lowest dγ level for the metal ions at the surface, the occupation of all the dγ levels must be below unity in order to have a partially empty d_{z^2} level. In the present system, the Mn^{4+} ions ($3d^3$) had only one type of the electron configuration with $(d\varepsilon)^3(d\gamma)^0$, and the Mn^{3+} ions ($3d^4$) had the electron configurations of both the low-spin state with $(d\varepsilon)\,^4(d\gamma)^0$ and the high-spin state with $(d\varepsilon)^3(d\gamma)^1$ [3]. The electron configurations with $(d\varepsilon)^3(d\gamma)^0$, $(d\varepsilon)^4(d\gamma)^0$, and $(d\varepsilon)^3(d\gamma)^1$ have the partially empty d_{z^2} level. Therefore, it is considered that both the Mn^{4+} and the Mn^{3+} ions have a high catalytic activity. With increasing Al^{3+} ion content, the catalytic activity increased and had a maximum value at the average valence of the Mn^{4+} and Mn^{3+} ions in analogy with the perovskite-type oxides.

It is concluded that murdochite-type $(Mg_{6-x}Al_x)$-MnO_8 ($0 \leqslant x \leqslant 0.6$) was synthesized at 700 °C with the sol–gel process. The specific surface area of the samples increased with increasing Al^{3+} ion content, and this increase was explained by the decrease of the crystallite size. The increase of the catalytic activity was correlated with the electron configuration of the manganese ions, that is, it was caused with the valence deviation of the manganese ions.

References

1. J. S. KASPER and J. S. PRENER, *Acta Crystallogr.* **7** (1954) 246.
2. P. PORTA and M. VALIGI, *J. Solid State Chem.* **6** (1973) 34.
3. H. TAGUCHI, A. OKAMOTO, M. NAGAO and H. KIDO, *ibid.* **102** (1993) 570.
4. A. CIMINO and V. INDOVINA, *J. Catal.* **17** (1970) 54.

5. H. TAGUCHI and M. NAGAO, *J. Mater. Sci. Lett.* **10** (1991) 658.
6. H. TAGUCHI, D. MATSUDA, M. NAGAO, K. TANIHATA and Y. MIYAMOTO, *J. Am. Ceram. Soc.* **75** (1992) 201.
7. Y. OKIGNO, T. ONODA, S. SHIKAGAWA, M. KARUBE, Y. SAITO, K. TABE, T. TAMURA, H. MATSUMOTO, M. MISONO and K. YOSHIDA, "Catalysis" (Maruzen, Tokyo, 1986) p. 880.
8. R. H. VOORHOEVE, D. W. JOHNSON, J. P. REMEIKA and P. K. GALLAGHER, *Science* **195** (1977) 827.
9. L. G. TEJUCA, J. G. FIERRO and J. M. D. TASCON, *Adv. Catal.* **36** (1989) 237.
10. T. NITADORI, S. KURIHARA and M. MISONO, *J. Catal.* **98** (1986) 221.
11. K. TABATA, I. MATSUMOTO and S. KOHIKI, *J. Mater. Sci.* **22** (1987) 1882.
12. T. NITADORI, T. ICHIKI and M. MISONO, *Bull. Chem. Soc. Jpn.* **61** (1988) 621.
13. N. MIZUNO, M. TANAKA and M. MISONO, *J. Chem. Soc. Farad. Trans.* **88** (1992) 91.

Received 6 March 1995
and accepted 8 May 1996